NATIONAL ADVISORY COMMITTEE FOR AERONAUTICS

TECHNICAL NOTE

No. 1420

AN APPLICATION OF LIFTING-SURFACE THEORY TO THE PREDICTION OF ANGLE-OF-ATTACK HINGE-MOMENT PARAMETERS FOR ASPECT RATIO 4.5 WINGS

By Arthur L. Jones, Mildred G. Flanagan, and Loma Sluder

Ames Aeronautical Laboratory
Moffett Field, Calif.

Washington
September 1947

NATIONAL ADVISORY COMMITTEE FOR AERONAUTICS

TECHNICAL NOTE NO. 1420

AN APPLICATION OF LIFTING-SURFACE THEORY TO THE PREDICTION OF ANGLE-OF-ATTACK HINGE-MOMENT PARAMETERS FOR ASPECT RATIO 4.5 WINGS

By Arthur L. Jones, Mildred G. Flanagan, and Loma Sluder

SUMMARY

An investigation has been made of the angle-of-attack-type loading for an elliptical wing of aspect ratio 4.5 in an attempt to augment the existing methods of prediction of finite span angle-of-attack hinge-moment parameters.

The angle-of-attack-type loading yields a linear variation of downwash from the 0.1 to the 0.9 chord station. In previous investigations this linear variation was extrapolated to cover the whole chord. In the present study, special consideration was given to the calculation of the vertical induced flow near the leading and trailing edges. Deviations from the linear downwash variation were found in these vicinities.

Despite the differences noted in the vertical induced velocity variations, application of these downwash results to the prediction of hinge-moment parameters produced results that compared well with the predicted values from previous investigations and with experimental results.

INTRODUCTION

The presentation of a semigraphical method of induced velocity calculation by Cohen (reference 1) led to the development of a lifting-surface-theory analysis of the variation of hinge moment with angle of attack for a finite span wing (reference 2). Subsequent analyses on an electro-magnetic-analogy model (reference 3) combined with the results of reference 1 produced a satisfactory method of predicting finite span hinge-moment parameters (reference 4). This method, however, is based upon a study of a limited number of aspect ratios and upon the assumption of a linear variation in downwash near the leading and trailing edges of the

wing. Consequently, the method and results of reference 4 are subject to possible changes as more extensive research in this field is completed.

This report covers the investigation of an angle-of-attack-type loading on a wing of elliptical plan form of aspect ratio 4.5 having a straight and unswept quarter-chord line. The predictions of the angle-of-attack parameters in reference 4 were based on calculations for wings of elliptical plan forms of aspect ratios 3 and 6 having a straight 50-percent-chord line. A different aspect ratio and a slightly different plan form, therefore, have been considered in this report. In particular, however, considerable progress toward a conclusive determination of the induced velocities near the leading and trailing edges has resulted from this investigation.

Differences with respect to previous results have been evaluated by comparison of these computations with the interpolated results of reference 4. Both sets of results have also been compared with experimental data from tests of four semispan horizontal-tail models.

SYMBOLS AND COEFFICIENTS

α	geometric angle of attack of lifting surface, degrees (unless otherwise specified)
α_i	induced angle of attack, degrees (unless otherwise specified)
C_L	lift coefficient
c_l	section lift coefficient
C_h	hinge-moment coefficient
c_h	section hinge-moment coefficient
c	chord of lifting surface at any section
c_0	chord in the plane of symmetry
$\overline{c}_f$	root-mean-square chord of the control surface
x/c	distance along the chord measured from the local leading edge as a fraction of the chord

$b/2$	semispan of the lifting surface
$\frac{y}{b/2}$	distance along the span divided by the semispan, measured from the plane of symmetry
b_f	total span of the control surface
C_{L_α}	variation of lift coefficient with angle of attack $(\partial C_L/\partial\alpha)$
c_{l_α}	variation of section lift coefficient with angle of attack $(\partial c_l/\partial\alpha)$
C_{h_α}	variation of hinge-moment coefficient with angle of attack $(\partial C_h/\partial\alpha)$
c_{h_α}	variation of section hinge-moment coefficient with angle of attack $(\partial c_h/\partial\alpha)$
q	free-stream dynamic pressure
w	vertical component of induced velocity
Δw	difference between the two- and three-dimensional induced velocities
Γ	circulation strength
Γ_{max}	maximum value of circulation strength on the surface
$\overline{\Gamma}$	average circulation strength around a circle of radius r
$\frac{w\ b/2}{\Gamma_{max}}$	nondimensional value of the vertical induced velocity
r	radial distance from a point in the plane of the lifting surface at which the induced velocity is being determined
A	aspect ratio
ΔP	the pressure coefficient, in terms of q, representing the difference in pressure between the upper and lower airfoil surface

METHOD

Determination of the Induced Velocities

The basis of the analytical phase of this investigation is the Cohen semigraphical lifting-surface method for induced velocity calculations (reference 1). By use of this method a two-dimensional chord loading, distributed over a finite span wing according to the dictates of lifting-line theory, can be analyzed with respect to satisfying the boundary conditions. Revisions to the assumed loading can be estimated from the discrepancies between the computed downwash and the known boundary conditions (usually the slope of the mean camber line). These revisions in loading are used to estimate three-dimensional-flow effects on the surface load distribution and the hinge-moment characteristics.

Previous work in the field of hinge-moment prediction has been based on downwash calculations from both the Cohen method and an electro-magnetic-analogy-model method (reference 3). The downwash results used in reference 2 were obtained from reference 1 which presented the downwash for only the one-quarter and three-quarter chord stations. The downwash results from the electro-magnetic-analogy model were presented only for values of x/c between 0.1 and 0.9 of the chord, since by the very nature of the equipment involved, the results nearer the leading and trailing edges could not be obtained.

By replacing some of the graphical operations with analytic methods it was possible to apply the Cohen method with considerable accuracy in regions that previously have been relatively unexplored. In particular, for radii from the point at which the downwash was sought up to an $\frac{r}{b/2}$ of approximately 0.1, the values of the circulation Γ were determined analytically, not graphically, and considerably more accurate values of Γ for the smaller radii were obtained in this manner.

The leading-edge points received special consideration. A modification covering the first 1-1/4-percent chord was made to the vorticity distribution of the thin airfoil additional loading, shown in figure 1, to obtain a more amenable solution for the leading-edge induced velocity. A quartic of the type $A + B\,(x/c)^2 + C\,(x/c)^4$ was substituted, having $\frac{d\Gamma}{d(x/c)} = 0$ at $x/c = 0$. At the 1-1/4-percent-chord station the ordinate and slope of both the original and quartic curves were made equal

as shown in figure 2. The effect of this revision on the assumed chordwise load distribution was merely to make the value of the load at the leading edge zero rather than infinity and to alter the pressure distribution for the 1-1/4 percent of chord over which the revision extended. The revision of the Γ curve had a large effect on the values of the induced velocities at the leading edge (fig. 3), but their effect on the quarter- and three-quarter-chord velocities was negligible. As the chord correction results are based on the difference between the two-dimensional and three-dimensional induced velocities, moreover, these results are as generally applicable to the angle-of-attack hinge-moment parameters as are results using the theoretical angle-of-attack chord loading.

The assumption of a unit maximum circulation and a unit semispan (as done in reference 1) yielded solutions for the downwash in a nondimensional form as $\frac{w\ b/2}{\Gamma_{max}}$. Values of the induced velocities for the chordwise and spanwise stations investigated on the aspect ratio 4.5 wing are given in table I. These results were compared with the induced velocity at the corresponding chordwise stations for the two-dimensional flow, and the increments $\Delta \frac{w\ b/2}{\Gamma_{max}}$, shown in figure 4, were determined.

Determination of the Load and Hinge-Moment Corrections

In general, to convert the velocity increments into load increments, an average induced angle of attack is assumed that corresponds closely to the mean value of the induced velocity increments on the wing. The load resulting from this average induced angle of attack merely changes the magnitude of the chordwise load distribution assumed and therefore corresponds to the usual lifting-line-theory type of correction. For the prediction of C_{h_α} this part of the correction takes the form

$$C_{h_\alpha} = \left(\frac{\alpha - \alpha_i}{\alpha}\right) c_{h_\alpha} \qquad (1)$$

if the spanwise integration can be neglected. The remaining induced velocities yield a load correction composed partly of additional-type loading and partly of a camber-type loading that can be evaluated by the methods of reference 5. This load correction can be converted to a hinge-moment correction Δc_h by integration over the control-surface chord.

These additive streamline-curvature hinge-moment corrections can be considered either as corrections per unit lift coefficient or as corrections per unit geometric angle of attack if the section results are multiplied by the section lift-curve slope. If the correction is assumed to be per unit lift coefficient, it is sufficient to multiply by the finite-span lift-curve slope C_{L_α} to account for the effects of aerodynamic induction in the conversion of the integrated hinge-moment correction to ΔCh_α.

$$\Delta Ch_\alpha = \Delta\left(\frac{\partial C_h}{\partial C_L}\right) C_{L_\alpha} = \frac{C_{L_\alpha}}{(b_f/b)\ (\overline{c}_f)^2}\int_0^1 \Delta\left(\frac{\partial c_h}{\partial c_l}\right) c_f^2\, d\left(\frac{y}{b/2}\right) \qquad (2)$$

To evaluate the differences between the results of reference 4 and this report, while keeping the approximate factors to a minimum, comparisons of the hinge-moment parameters were made on the basis of the unit lift coefficient. Equation (13) of reference 4 and equation (2) in this report were used to get the integrated results over the span of the wing. In order to obtain a more practical evaluation of the differences in hinge moment, comparisons were made of both sets of results with experimental values of Ch_α for four semispan horizontal-tail models. The geometric characteristics of these models are presented in table II. The plan forms and airfoil profiles of these models are sketched in figure 5.

The procedure used in reference 4 to convert $\Delta(\partial C_h/\partial C_L)$ to ΔCh_α is more rigorous in accounting for induced effects than the procedure used herein. In addition, reference 4 includes a factor η which is intended as a viscosity correction to the streamline curvature load. These factors had very little effect for the cases considered in this investigation, but the effect of the η factor can become appreciable for airfoil profiles having sizable trailing-edge angles.

RESULTS AND DISCUSSION

Comparison of Downwash Results With Interpolated Downwash From Reference 4

The variation of $\Delta \frac{w\ b/2}{\Gamma_{max}}$ along the chord is shown in figure 4 for the center line, 0.5 b/2 and 0.9 b/2 spanwise stations of the elliptic wing of aspect ratio 4.5. Curves are included also for elliptical plan forms of aspect ratios 3 and 6 from reference 4.

At the center line and 0.5 b/2 spanwise stations the downwash results for the aspect ratio 4.5 correspond fairly well, except at the leading edge, to what might be expected from an interpolation between the aspect ratios 3 and 6 results of reference 4. Close examination reveals, however, that small but possibly effective differences exist. The slope of the downwash at 0.5 b/2 is slightly greater than a reasonable interpolation might yield, and near the trailing edge a slight departure from the linear slope can be noted. At 0.9 b/2 the slope of the greatest extent of the curve is slightly greater than the probable interpolated value. The curvature in the downwash variation near the trailing edge has become marked, however, and the over-all values of the downwash are greater than the values for aspect ratios 3 or 6 and, consequently, are greater than any possible interpolated values for the aspect ratio 4.5.

The tendency of the induced velocities to diminish in magnitude near the trailing edge is merely an early manifestation of the trend of the downwash to return to a value of $0.5 \frac{w\ b/2}{\Gamma_{max}}$ at an infinite distance behind the wing. In terms of the load distribution, it is an indication that the load in the vicinity of the trailing edge must be increased to satisfy the boundary conditions locally.

The increase in the average value of the downwash at the 0.9 b/2 station over the values from reference 4 must be attributed to plan-form effects (in this case the difference between a linear quarter-chord line or a linear 50-percent-chord line) until more extensive induced velocity analyses are carried out for elliptical plan forms.

Effects of the Chordwise Downwash Differences on the Hinge-Moment Parameters

By converting the downwash results to chord loading curves and hinge-moment parameters, the effect of these differences of induced velocities was evaluated.

The influence of the nonlinearity of the chordwise induced velocity variation near the leading edge was not expected to be very great on the distribution of the pressure over the rear part of the chord. This expectation was confirmed by comparison of the combined induced angle of attack and streamline curvature chord loadings over the rear half of the chord for both an extrapolation

of the linear slopes and the actual curves containing the arbitrary fairing to the leading-edge points. Consequently, no further consideration was given to these leading-edge values and, for the region forward of the quarter chord, the curves were assumed to be extensions of the linear slope in the subsequent calculations.

The slight increase in load over the rear part of the chord due to the reduction of the downwash in that vicinity tends to yield more negative hinge moments. At 0.9 b/2 this tendency is counteracted by the increase in the average value of downwash which yields an algebraically positive hinge-moment correction. At 0.5 b/2 the slightly greater value of the negative slope of the downwash curve tends to counteract the effect of the reduction in downwash near the trailing edge. To estimate the accumulated effect of these changes on the hinge moment, an elliptical plan form with a 30-percent-chord plain flap was selected, and values of the parameter $\Delta\partial c_h/\partial c_L$ were computed. Comparisons were made of the value of $\Delta\partial c_h/\partial c_L$ obtained from reference 4, the value corresponding to the extended linear slopes and the value corresponding to the downwash variation containing the curvature between $x/c = 0.95$ and $x/c = 1.00$. The results are given in the following table:

Source	$\Delta\partial c_h/\partial c_L$
Reference 4	0.0162
Linear downwash variation	0.0206
Nonlinear downwash variation	0.0186

The effects of the increased slope of the downwash curve at 0.5 b/2 and the increase in the average value of the downwash at 0.9 b/2 have more than compensated for the effect of the curvature in the downwash variation near the trailing edge. The net increment in $\Delta\partial c_h/\partial c_L$ that this investigation yields over that given by reference 4 is 0.0024 which corresponds to a Δc_{h_α} of approximately 0.00016 for an aspect ratio of 4.5. Since the total correction to c_{h_α} is about $\Delta c_{h_\alpha} = 0.0012$, this possible error of approximately 10 percent does not appear to be large enough to invalidate the hinge-moment-prediction results in reference 4. Indeed, a comparison of both sets of analytical results with the experimental results for the four semispan horizontal tails of aspect ratio 4.5 affirms this conclusion. The predicted and experimental values of c_{h_α} shown in table III are in excellent

agreement with the exception of the value for Ch_α predicted for model A, using reference 4. This model had a constant-chord control surface, and in applying reference 4 it was necessary to use averaged values of the parameters that varied along the span; whereas, the predicted value for model A based on the results from this investigation was obtained by a spanwise integration and yielded a suitable prediction.

Status of Hinge-Moment Prediction Methods

In general the present and previous comparisons with experimental results have indicated that reference 4 yields suitable predictions for simple conventional control-surface configurations when the section data were known or could be estimated readily. For control surfaces having unusual features such as horn balance, large cutouts, profiles that differ greatly from the standard subsonic profiles, etc., the predictions using reference 4 might not be sufficiently accurate. The possible variations in such factors as plan form, aerodynamic balance, viscosity effects and section profile are so numerous that an analysis involving the effects of all these factors appears to be impossible. However, a reasonable estimation of the effects of the most important parameters as presented in reference 6 for airfoil sections and in reference 4 for three-dimensional wings should suffice for general application. Further investigations covering three-dimensional effects, such as carried out herein, may possibly add improvements to the general method. It is probable, however, that further improvements in hinge-moment prediction will be restricted to specific three-dimensional configurations and to the more comprehensive analysis of the airfoil section parameters with regard to two-dimensional hinge-moment data.

CONCLUDING REMARKS

The downwash results from this investigation of an aspect ratio 4.5 elliptical wing agree in general with the downwash results from previous investigations. The previously established linearity of the downwash variation along the chord, however, was not verified near the leading and trailing edges.

The trailing edge nonlinearity had an appreciable effect on the correction to the chordwise load distribution but, due to an accumulation of other minor downwash differences, this effect of the nonlinearity was counteracted to a considerable degree.

The net effect of the differences between the downwash results for this and previous investigations was studied by comparison of predicted values of Ch_α with the experimental values for four semispan horizontal-tail models. These comparisons indicated that in such practical applications the results of this and the previous investigation agreed well with the experimental results and with each other.

Ames Aeronautical Laboratory,
National Advisory Committee for Aeronautics,
Moffett Field, Calif.

REFERENCES

1. Cohen, Doris: A Method for Determining the Camber and Twist of a Surface to Support a Given Distribution of Lift. NACA TN No. 855, 1942.

2. Swanson, Robert S., and Gillis, Clarence L.: Limitations of Lifting-Line Theory for Estimation of Aileron Hinge-Moment Characteristics. NACA CB No. 3L02, 1943.

3. Swanson, Robert S., and Crandall, Stewart M.: An Electromagnetic-Analogy Method of Solving Lifting-Surface-Theory Problems. NACA ARR No. L5D23, 1945.

4. Swanson, Robert S., and Crandall, Stewart M.: Lifting-Surface-Theory Aspect-Ratio Corrections to the Lift and Hinge-Moment Parameters for Full-Span Elevators on Horizontal Tail Surfaces. NACA TN No. 1175, 1947.

5. Naiman, Irven: Numerical Evaluation of the ϵ-Integral Occurring in the Theodorsen Arbitrary Airfoil Potential Theory. NACA ARR L4D27A, 1944.

6. Crane, Robert M.: Computation of Hinge-Moment Characteristics of Horizontal Tails from Section Data. NACA CB No. 5B05, 1945.

TABLE I

THE COMPUTED VALUES OF VERTICAL INDUCED VELOCITY $\frac{w\ b/2}{\Gamma_{max}}$ FOR THE FINITE AND INFINITE ASPECT RATIOS

Chordwise station, x/c	Infinite aspect ratio	Aspect ratio 4.5		
		$\frac{y}{b/2} = 0$	$\frac{y}{b/2} = 0.5$	$\frac{y}{b/2} = 0.9$
0	-10.650	-10.440	-10.532	-10.930
.25	.562	.832	.834	.825
.75	do.	.875	.892	1.001
.80	do.	.876	— —	— —
.85	do.	— —	— —	1.033
.95	do.	.885	.911	1.068
.99	do.	— —	— —	1.053
1.00	.562	.890	.910	1.039

NATIONAL ADVISORY
COMMITTEE FOR AERONAUTICS

TABLE II

THE GEOMETRIC CHARACTERISTICS OF THE FOUR SEMI-SPAN HORIZONTAL TAIL MODELS INVESTIGATED

Geometric characteristics	Horizontal-tail models			
	A	B	C	D
Aspect ratio	4.5	4.5	4.45	4.5
Taper ratio	0.5	0.5	0.5	0.5
Elevator chord	.25c(av.)	.27c	.33c	.41c
Balance chord	$.12c_f$(av.)	$.15c_f$	$.15c_f$	$.43c_f$
$\frac{b_f}{b/2}$	1.0	1.0	.92	.872

NATIONAL ADVISORY
COMMITTEE FOR AERONAUTICS

TABLE III

THE PREDICTED AND EXPERIMENTAL VALUES OF C_{h_α} FOR AN ASPECT RATIO OF 4.5

Semispan horizontal tail model	Aspect ratio	Lifting-line theory, C_{h_α}	Correction to lifting-line theory, ΔC_{h_α}	Lifting-line theory plus correction, C_{h_α}	C_{h_α} (Reference 4)	C_{h_α} (Experimental)	Error (Lifting-line theory)	Error (Lifting-line theory plus correction)	Error (Reference 4)
A	4.5	-0.0038	0.0016	-0.0022	-0.0031	-0.0022	-0.0016	0	-0.0009
B	4.5	-.0019	.0008	-.0011	-.0011	-.0011	-.0008	0	0
C	4.45	-.0022	.0010	-.0012	-.0014	-.0014	-.0008	.0002	0
D	4.5	-.0008	.0006	-.0002	-.0001	-.0001	-.0007	-.0001	0

NATIONAL ADVISORY
COMMITTEE FOR AERONAUTICS

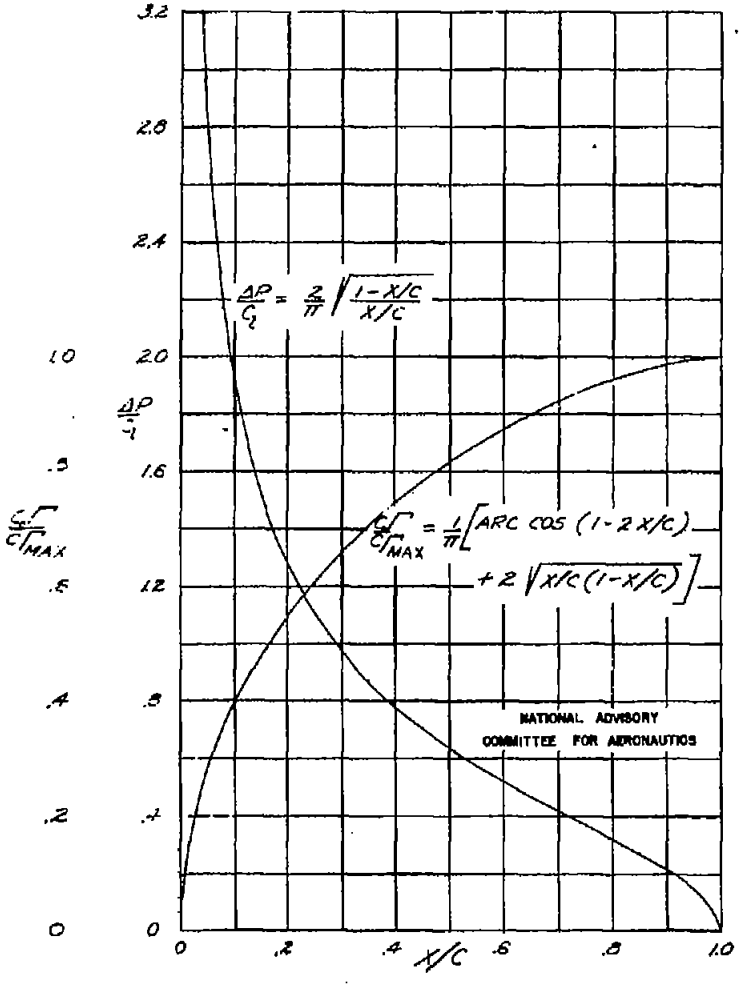

FIGURE 1.- THE THIN AIRFOIL ADDITIONAL CHORDWISE LIFT DISTRIBUTION AND THE CHORDWISE CIRCULATION DISTRIBUTION CORRESPONDING TO THE INTEGRATION OF THE CHORDWISE LIFT.

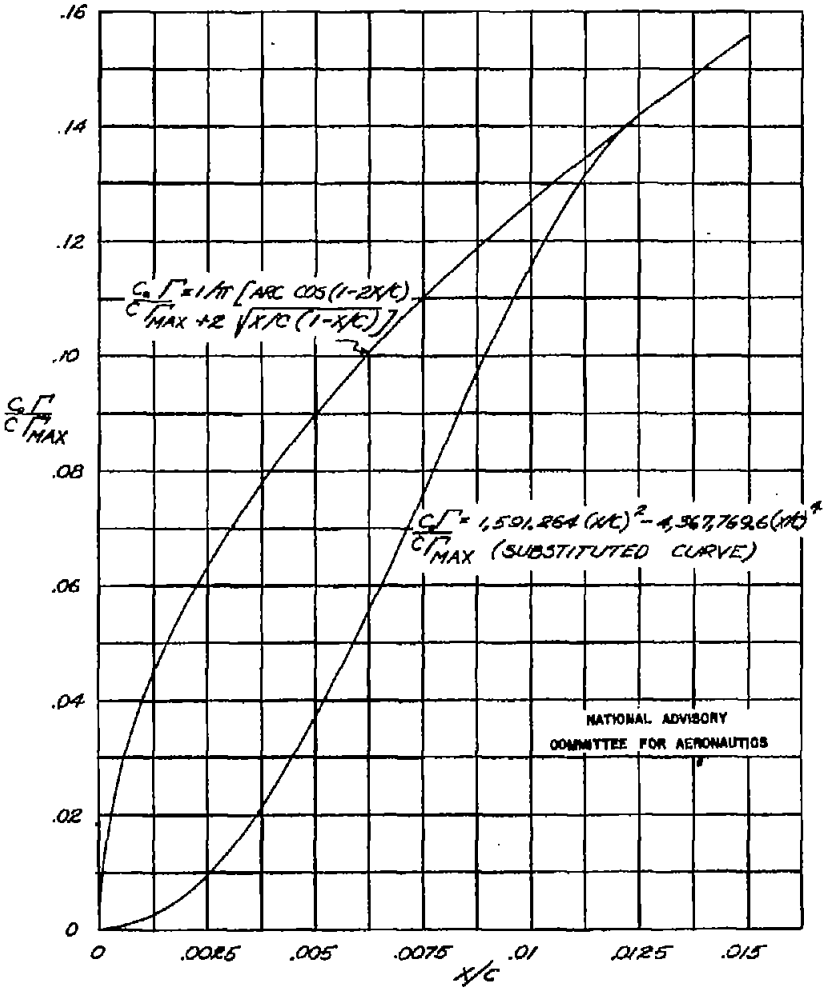

FIGURE 2.- A PORTION OF THE CHORDWISE CIRCULATION DISTRIBUTION NEAR THE LEADING EDGE AND THE FOURTH DEGREE CURVE THAT WAS SUBSTITUTED TO OBTAIN $d\Gamma/d(X/C) = 0$ AT $X/C = 0$.

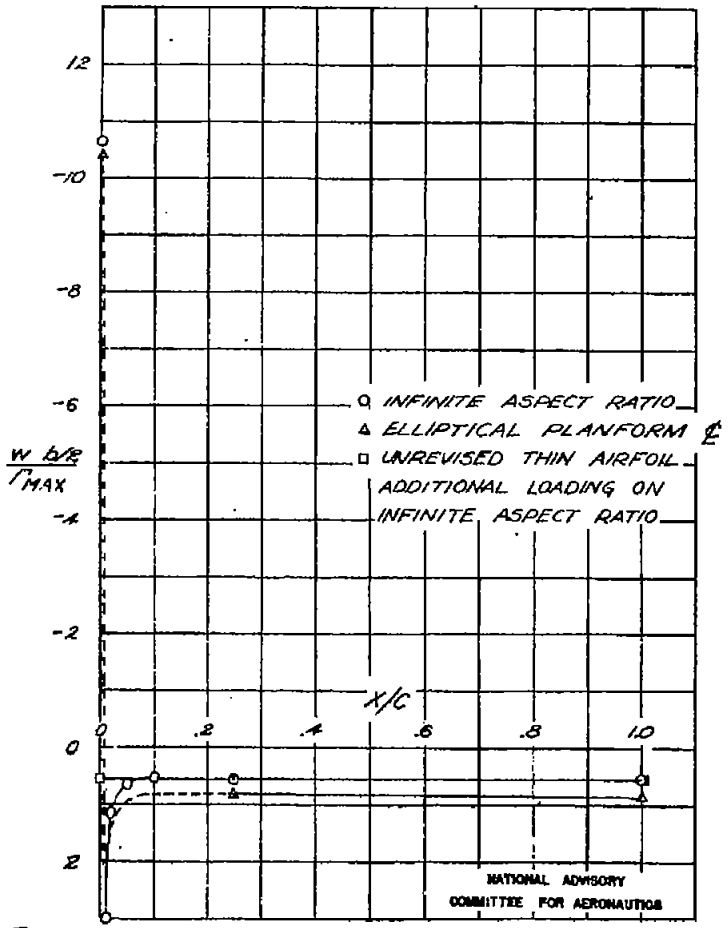

FIGURE 3.- THE RELATIVE VALUES OF THE VERTICAL INDUCED VELOCITIES ALONG THE CHORD OF THE INFINITE ASPECT RATIO PLANFORM AND ALONG THE CHORD AT THE CENTER LINE OF THE ELLIPTICAL PLANFORM FOR THE CHORDWISE LOADING APPLIED.

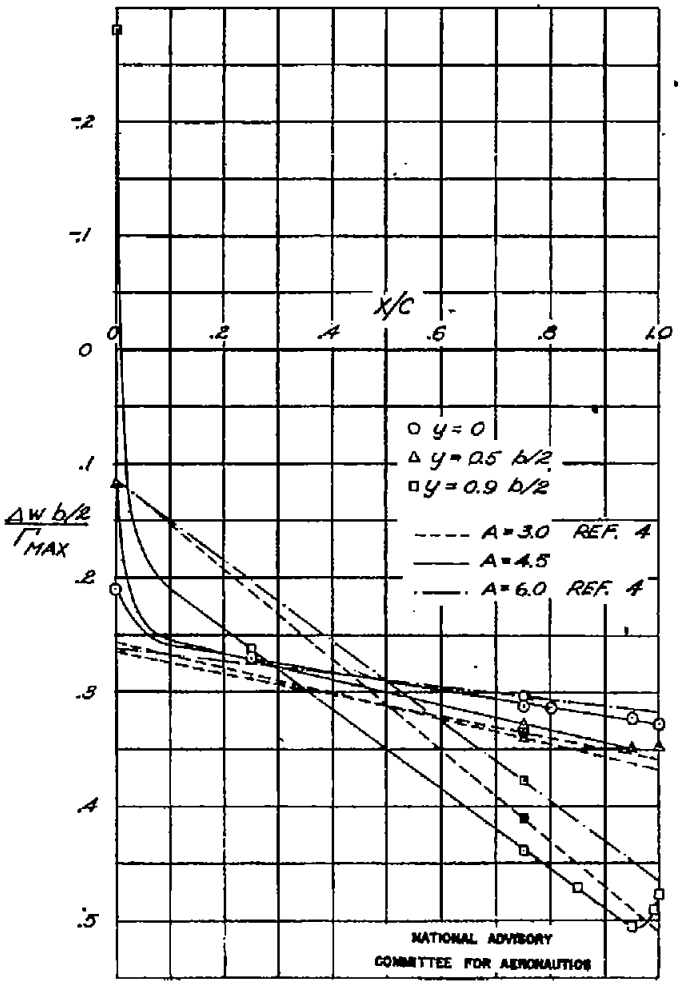

FIGURE 4.- THE CHORDWISE VARIATION AT THREE STATIONS ALONG THE SPAN OF THE CHANGE IN VERTICAL INDUCED VELOCITY WHICH IS DUE TO A CHANGE IN PLANFORM FROM INFINITE ASPECT RATIO TO ELLIPTICAL PLANFORMS HAVING ASPECT RATIOS OF 3.0, 4.5 AND 6.0.

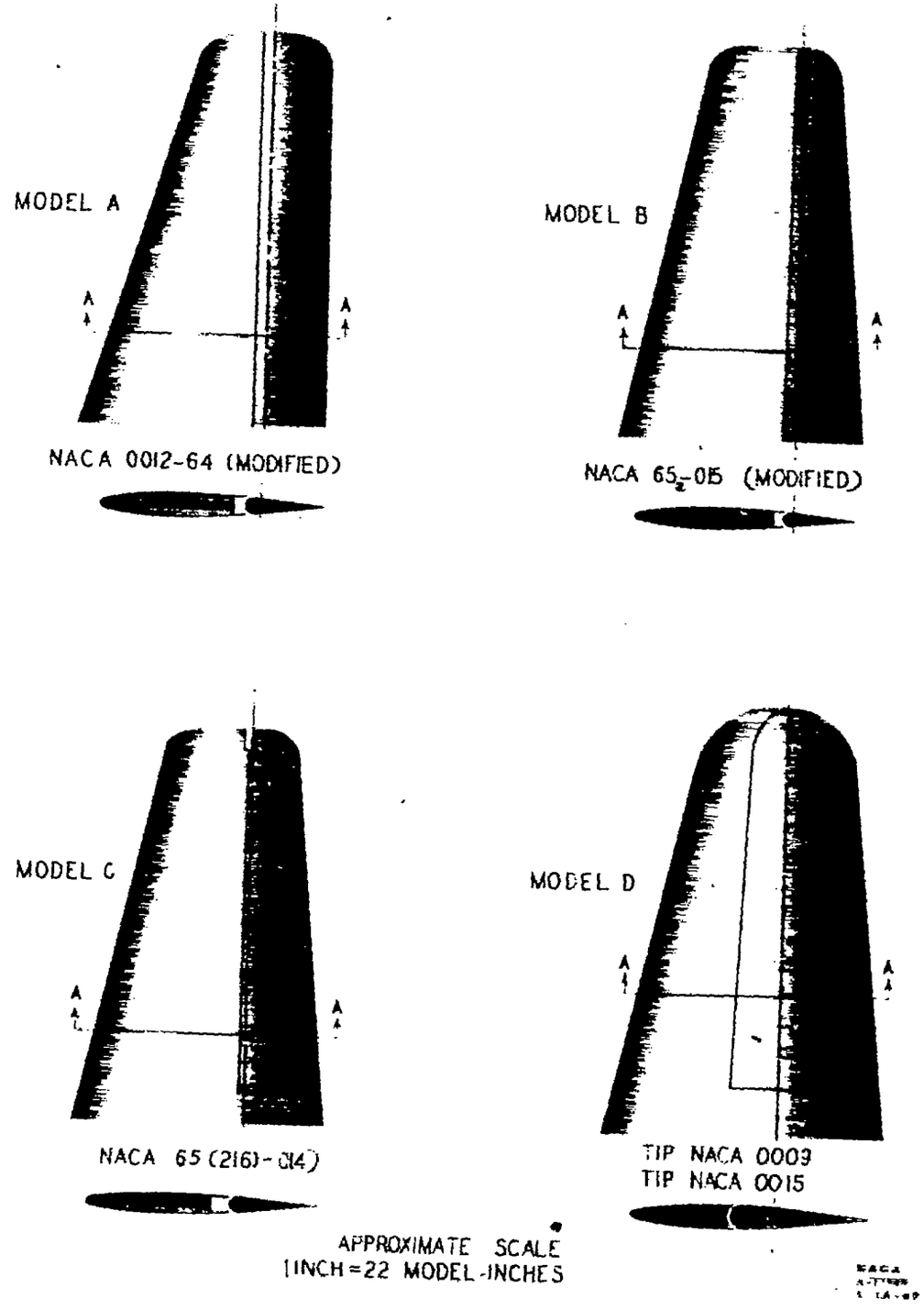

Figure 5.- Plan forms and profiles of the four semispan horizontal tail models.